Fenton and solar photo-Fenton processes for the removal of chlorpyrifos insecticide in wastewater

Youssef Samet*, Emna Hmani and Ridha Abdelhédi

UR Electrochimie et Environnement , Department of Materials Engineering, National Engineering School of Sfax, BPW 3038 Sfax, University of Sfax, Tunisia

Abstract

The degradation of chlorpyrifos in water by Fenton (H_2O_2/Fe^{2+}) and solar photo-Fenton (H_2O_2/Fe^{2+}/solar light) processes was investigated. A laboratory-scale reactor was designed to evaluate and select the optimal oxidation condition. The degradation rate is strongly dependent on pH, temperature, H_2O_2 dosing rate, and initial concentrations of the insecticide and Fe^{2+}. The kinetics of organic matter decay was evaluated by means of chemical oxygen demand (COD) measurement. Overall kinetics can be described by a pseudo-second-order rate equation with respect to COD. The optimum conditions were obtained at pH 3, H_2O_2 dosing rate 120 mg·min^{-1}, $[Fe^{2+}]_0$ 5.0 mM, initial COD 1 330 mg·ℓ^{-1} and 35°C for the Fenton process. However, in the solar photo-Fenton process, the degradation rate increased significantly. To achieve 90% of COD removal, the solar photo-Fenton process needs 50% less time than that used in the Fenton process which translates to a 50% gain of H_2O_2.

Keywords: chlorpyrifos; degradation kinetic; Fenton; solar photo-Fenton; COD removal

Introduction

The use of insecticides, herbicides, fungicides, etc., grouped under the name of pesticides, has led to improved yields and diversity of crops to meet the nutritional demand related to the increase in world population. However, this use has also had indirect and harmful effects on the environment. Studies have shown the presence of pesticide residues in food (Cunnif, 1995), groundwater and surface water (Di Corcia and Marchetti, 1992). Various technologies have been proposed for the removal of pesticides from water. Conventional techniques, such as physical methods of mass transfer (flocculation, filtration, precipitation, adsorption onto active charcoal, etc.), incineration, or the biological pathway, are either ineffective in the face of the extent of this pollution, or result in crippling costs, or are a source of secondary pollution (sludge formation); hence there is a need to seek better alternatives.

In this context, advanced oxidation processes (AOPs) have considerable potential for becoming feasible alternatives for the remediation of contaminated wastewater. AOPs are based on the generation and subsequent reactions of hydroxyl radicals (OH·). These are short-lived, powerful oxidising agents, which react by second-order kinetics with the majority of organic substances with low selectivity (Esplugas et al., 2002). OH· are produced *in situ* by chemical, electrochemical and/or photochemical reactions in AOP systems.

Among many AOPs, Fenton (H_2O_2/Fe(II)) and solar photo-Fenton treatment processes (combination of H_2O_2, Fe(II) and solar irradiation) have been proven to be effective in degradation and mineralisation of single organic toxicants and the mixtures of various organic wastes (Xu et al., 2007).

The photo-Fenton process can be divided into the following stages (Pignatello, 1992; Bossmann et al., 1998): the first step is the so-called Fenton reaction, in which ferrous ions are oxidised to ferric ions in acidic aqueous solution, as shown in Eq. (1), giving rise to hydroxyl radicals:

$$Fe^{2+} + H_2O_2 \rightarrow Fe^{3+} + OH^- + OH^· \qquad (1)$$
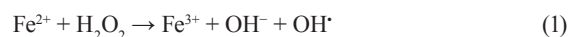
The ferric ions, represented by the complex $Fe(OH)^{2+}$, is reduced back to Fe^{2+} by UV-visible irradiation according to Eq. (2):

$$Fe(OH)^{2+} + hv \rightarrow Fe^{2+} + OH^· \ (\lambda < 450 \text{ nm}) \qquad (2)$$
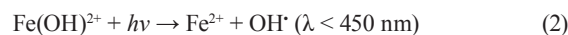
The ferric species can also form complexes with the initial organic compounds and/or degradation products, leading to photo-reduction back to Fe^{2+}, according to Eq. (3):

$$Fe(RCO_2)^{2+} + hv \rightarrow Fe^{2+} + R^· + CO_2 \ (\lambda < 500 \text{ nm}) \qquad (3)$$
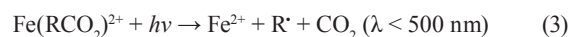
The OH· species formed will then attack the organic substrates present in the wastewater. Nevertheless, numerous competitive reactions can also occur, namely, the following, which negatively affect the oxidation process (Harber and Weiss, 1934; Walling, 1975; Kang and Hwang, 2000):

$$Fe^{2+} + OH^· \rightarrow Fe^{3+} + OH^- \qquad (4)$$
$$H_2O_2 + OH^· \rightarrow HO_2^· + H_2O \qquad (5)$$
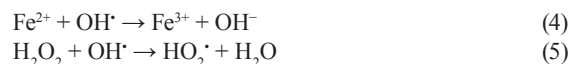
This network of consecutive and parallel reactions results in complex reaction kinetics. To overcome these difficulties, most of the kinetic studies focused on single component degradation or, in the case of complex effluents, the overall kinetics was analysed instead.

The use of Fenton and photo-Fenton processes in the treatment of pesticide-containing wastewater is a recent application. The degradation of triazine herbicides (Burrows et al., 2002), methylparathion (Chiron et al., 1999), fenuron (Acero et al., 2002) and diuron (Burrows et al., 2002) are known examples.
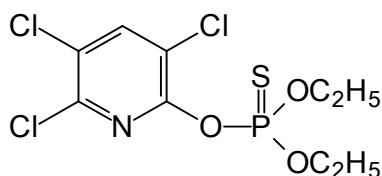
In this work, the efficiency of AOPs in the remediation of wastewater contaminated with the insecticide chlorpyrifos

---

*   To whom all correspondence should be addressed.
☎   (00216) 9866 0766; fax: (00216) 7427 4437;
    e-mail: youssef.samet@fss.rnu.tn

Figure 1
Chemical structure of chlorpyrifos

(Fig. 1), employed extensively in agriculture in Tunisia, was investigated in a laboratory-scale reactor. The effects of Fe^{2+} and chlorpyrifos concentrations, H_2O_2 dosing rate, pH and temperature were investigated in the case of the Fenton process and the optimum conditions were applied in the case of the solar photo-Fenton system.

It should be noted that the chlorpyrifos oxidation pathway using different AOPs, such as photo-Fenton (Murillo et al., 2010), ozonation (Meng et al., 2010), and electrochemical (Samet et al., 2010) AOPs, has been investigated. The main identified by-product is chlorpyrifos-oxon.
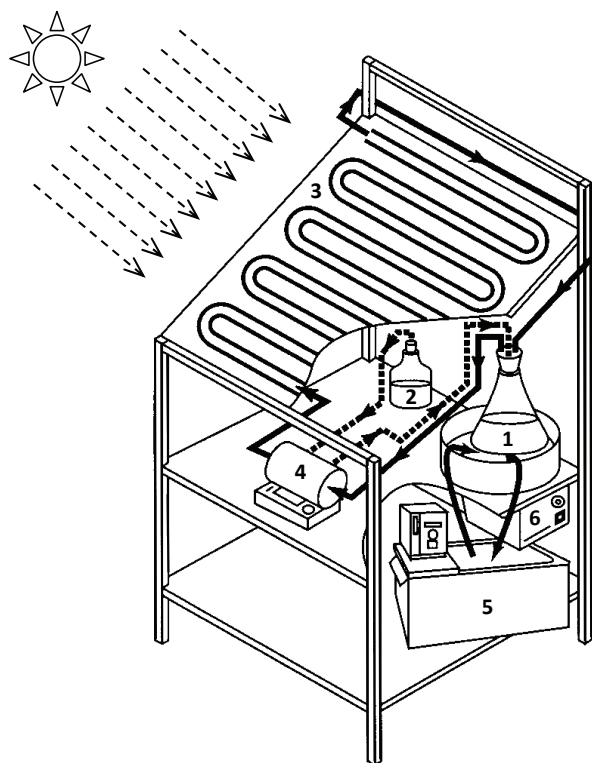
Experimental

A schematic view of the experimental device used in this work is shown in Fig. 2. All experiments were carried out with the same equipment. The equipment consisted of an aluminium frame (0.5 m length; 0.5 m width and 0.6 m height), which supports: (i) A platform of aluminium placed 34° to the horizontal and on which was fixed a solar reactor consisting of a borosilicate glass tube (4.5 m length, an inner diameter of 6 mm and outer diameter of 8 mm; and snake-shaped); and (ii) an Erlenmeyer flask (Pyrex 1 ℓ) in which the chlorpyrifos solution was prepared with bi-distilled water. This Erlenmeyer flask was immersed in a water bath in order to control the working temperature using a thermostat (Julabo Labortechnik GMBH, Sellback, Germany). The treated volume was 1 ℓ, and the solution was circulated through the reactor using a peristaltic pump (Cole-Parmer Instrument, Chicago, Illinois 60648 USA) with a flow rate of 140 mℓ·min⁻¹. This pump was simultaneously used to generate the flow of the H_2O_2 solution from the Erlenmeyer flask with a constant rate of 0.7 mℓ·min⁻¹. The ferrous sulphate was introduced into the solution at start-up. The solutions were continuously stirred using a magnetic stirrer (Tacussel, France).

The solar photo-Fenton experiments were performed at the Electrochemical and Environmental Laboratory, National Engineering School of Sfax (approximately 3 m amsl, latitude: 34° 44′ N, longitude: 10° 45′ E), Tunisia. All tests were conducted between 11:00 and 15:00 on sunny days from April to June 2010. The global solar radiation intensity was approximately 850 W·m⁻².

For tests using only the Fenton reagent, the experimental device was kept away from solar radiation by covering it with a black plastic film and aluminium foil.

Samples (0.5 mℓ) were withdrawn from the reactor at selected intervals for COD analysis. COD was measured using a spectrophotometer *(Shimadzu UV-Mini 1240 UV/Vis* Spectrophotometer) using a dichromate solution as the oxidant in strong acid media (Kolthof et al., 1969).

Since the residual H_2O_2 interferes with the measurement of COD (Kang et al., 2002), the residual amount of H_2O_2 was also measured, using the permanganate titration. This method is suitable for measuring solutions of hydrogen peroxide in the

Figure 2
Scheme of the experimental installation. (1) Erlenmeyer flask (chlorpyrifos solution); (2) H_2O_2 solution; (3) solar reactor; (4) peristaltic pump; (5) thermostatic bath; (6) magnetic stirrer.

range 0.25 to 70% wt (Lin and Lo, 1997). Correction of hydrogen peroxide interference was performed to COD analysis.

In this work, all solutions were prepared in the laboratory. These solutions contained quantities of chlorpyrifos taken from an emulsifiable concentrate (DURSBAN* 4, from Dow Agrosciences) containing 480 g·ℓ⁻¹ (44.6% W/W) chlorpyrifos. All of the solutions were freshly prepared with double-distilled water. Sulphuric acid of analytical grade was employed for pH adjustment. Ferrous sulphate heptahydrate ($FeSO_4$ $7H_2O$) was obtained from Riedel-de Haën (Seelze-Hannover, Germany) and used as the Fe(II) catalyst. Hydrogen peroxide (35% v/v) and sulphuric acid were provided by Merck (Darmstadt, Germany).

All samples were tested in duplicate, and the test was reproduced 3 times for each sample, so that the relative errors could be minimised. All of the figures show the average values.

Initial conditions (COD_0 = 465 mg·ℓ⁻¹ > 200 mg·ℓ⁻¹, $[Fe^{2+}]_0$ = 0.5 mM and H_2O_2 dosing rate = 30 mg·min⁻¹) were chosen after preliminary tests which lead to quantitative decrease in organic matter. A pHof 3 was chosen because Fenton or photo-Fenton processes require Fe^{2+} and Fe^{3+} ions. These species are more stable at this value of pH, as indicated by the Pourbaix diagram. At pH>3 Fe^{3+} will be precipitated to $Fe(OH)_3$. The ambient temperature, T, was 25°C.

## Results and discussion

Oxidation of chlorpyrifos by the Fenton process

Effect of the dosing rate of hydrogen peroxide

The dosing rate of H_2O_2 is considered to be one of the most important factors which should be considered in the Fenton
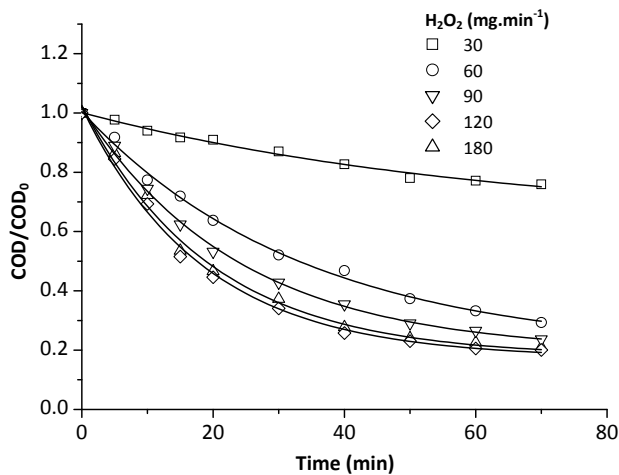
Figure 3
Effect of hydrogen peroxide dosing rate on the trend of COD/COD_0 ratio during the oxidation of chlorpyrifos solution by Fenton process. $[Fe^{2+}]_0 = 2.0$ mM; $COD_0 = 1\,330$ mg·ℓ⁻¹, pH = 3 and T = 25°C.
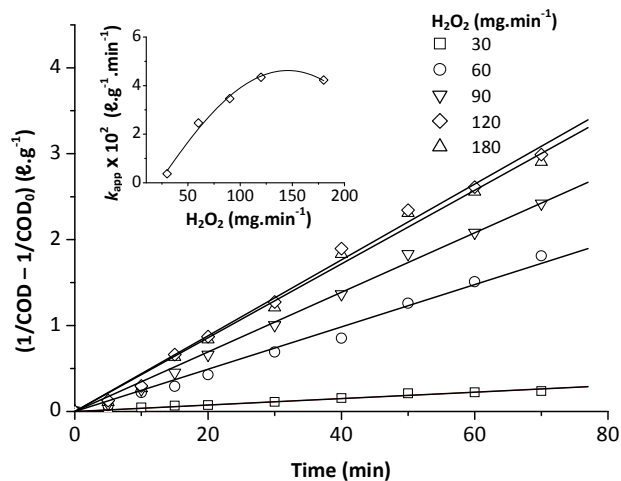
Figure 4
Plot of $(1/COD – 1/COD_0)$ versus time at different dosing rate of hydrogen peroxide. The inset panel shows k_{app} evolution at different dosing rate of H_2O_2. $COD_0 = 1\,330$ mg·ℓ⁻¹; $[Fe^{2+}]_0 = 2.0$ mM; pH = 3 and T = 25°C.

Table 1
Kinetic degradation by Fenton process

H_2O_2 (mg·min⁻¹)		30	60	90	120
Pseudo-first-order	R^2	0.9683	0.9514	0.9342	0.8942
Pseudo-second-order	R^2	0.9914	0.9927	0.9891	0.9818
k_{app} x 10^2 (ℓ·g⁻¹·min⁻¹)		0.37	2.46	3.46	4.34

process. The effect of the dosing rate of hydrogen peroxide on the efficiency of the oxidation process was investigated under the operating conditions ($COD_0 = 1\,330$ mg· ℓ⁻¹, $[Fe^{2+}]_0 = 2$ mM, pH = 3 and T = 25°C) (Fig. 3). It was found that COD removal efficiency increases with increasing the dosing rate of hydrogen peroxide from 30 mg·min⁻¹ to 180 mg·min⁻¹. The highest per cent removal of COD was attained at 70 min when using a H_2O_2 dosing rate of 120 mg·min⁻¹, so further addition of H_2O_2 is not necessary. Excessive H_2O_2 reacts with OH⁻ (Eq. (5)) competing with organic pollutants and consequently reducing treatment efficiency.

In all tests, the drop in COD was more significant during the first few minutes of the reaction, when the concentration of organic matter is high. This was clearly observed in the case of the 120 mg·min⁻¹ H_2O_2 dosing rate. The data presented in Fig. 3 clearly indicate that the pseudo-second-order model gives better prediction than the pseudo-first-order model for COD removal, as indicated by the higher regression coefficients (R^2) (Table 1).

It is worth noting that several authors have reported that the decaying profile of COD obtained by Fenton oxidation of organic molecules can follow pseudo-second-order kinetics (Guedes et al., 2003; Ratanatamskul and Auesuntrachun, 2009; Argun and Karatas, 2011; Derco et al., 2010).

If we suppose that the hydroxyl radical concentration is constant during treatment, the COD removal rate r can be given by the following equation:

$$r = -\frac{dCOD}{dt} = k\,[OH^\bullet]^\alpha\,COD^2 = k_{app}\,COD^2 \qquad (6)$$

where:
α is the reaction order related to the hydroxyl radicals
k is the real rate constant

k_{app} is the global apparent rate constant for COD removal.

Integration of this equation subject to the initial condition COD = COD_0 at $t = 0$ leads to the following equation:

$$\frac{1}{COD} - \frac{1}{COD_0} = k_{app}\,t \qquad (7)$$

In this case, a plot of $1/COD – 1/COD_0$ versus time in every experiment must lead to a straight line, with a slope = k_{app}. For example, Fig. 4 shows this plot related to Fig. 3.

The inset of Fig. 4 shows the variation of the apparent rate constant values, at different H_2O_2 dosing rates, calculated from the straight lines obtained when considering a pseudo-second-order reaction. k_{app} increased significantly when the dosing rate of H_2O_2 increased, due to the effect of the additional produced OH⁻ radicals, but above 120 mg·min⁻¹ H_2O_2 dosing rate, the improvement was not obvious. Hence, 120 mg·min⁻¹ H_2O_2 appears to be an optimal dosing rate.
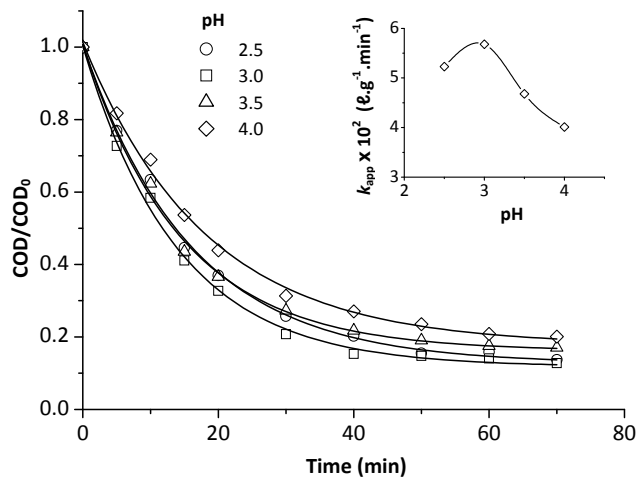
Effect of the initial chlorpyrifos concentration

The effect of chlorpyrifos concentration on the degradation efficiency was investigated at different initial concentrations (COD_0: 465, 825 and 1 330 mg·ℓ⁻¹), as presented in Fig. 5. It can be observed that the COD removal decreased with the increase of the initial concentration of the pollutant. Almost 90% of COD removal was achieved after about 40 and 60 min reaction time for COD_0 465 and 825 mg·ℓ⁻¹, respectively. Longer reaction time did not improve the COD per cent removal. However, at high chlorpyrifos concentrations the removal of COD requires more time and thus greater quantities of H_2O_2 (e.g. the per cent removal of COD is about 77% after 70 min when using $COD_0 = 1\,330$ mg·ℓ⁻¹). The reason for this is that when the concentration of chlorpyrifos increases, the quantity of hydroxyl radicals produced continuously with time does not increase accordingly; hence the removal rate decreases. Also, from the inset of Fig. 5 it can be seen that k_{app} decreased with COD_0. This behaviour was similar to that reported for other studies (e.g. Tamimi et al., 2008; Lucas and Peres, 2006; Modirshahla et al., 2007).
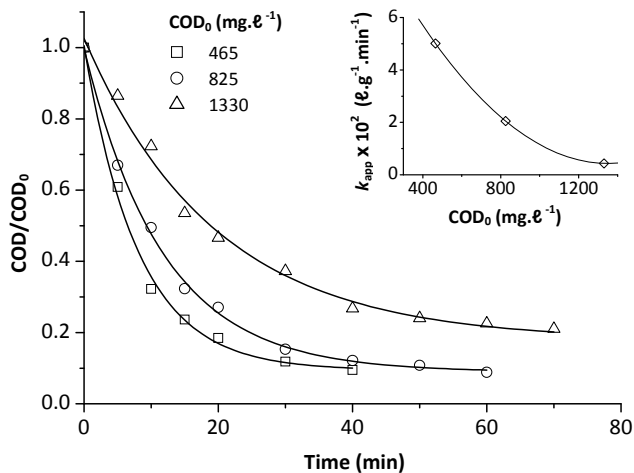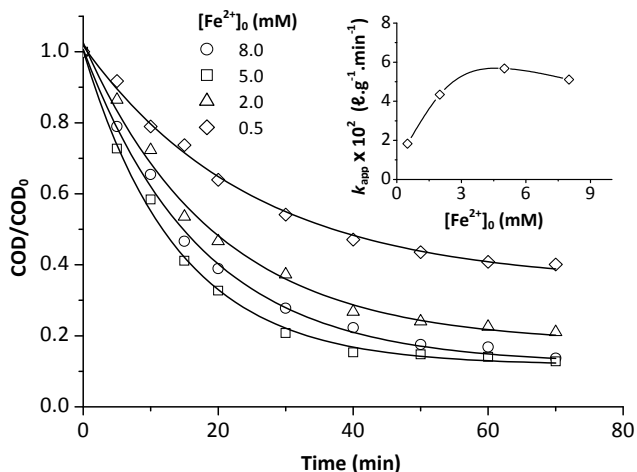
Figure 5
Effect of the initial concentration of chlorpyrifos on the COD removal by the Fenton process. The inset panel shows k_{app} evolution at different initial COD. Dosing rate of H_2O_2 120 mg·min^{-1}; $[Fe^{2+}]_0$ = 2.0 mM; pH = 3 and T = 25°C.

Figure 7
Effect of the initial pH on the COD removal by the Fenton process. The inset panel shows k_{app} evolution at different pH. Dosing rate of H_2O_2 120 mg·min^{-1}; $[Fe^{2+}]_0$ = 5.0 mM; COD_0 = 1 330 mg·ℓ$^{-1}$ and T = 25°C.

Figure 6
Effect of the initial concentration of Fe^{2+} on the COD removal by Fenton process. The inset panel shows k_{app} evolution at different Fe^{2+} concentrations. COD_0 = 1 330 mg·ℓ$^{-1}$; Dosing rate of H_2O_2 120 mg·min^{-1}; pH = 3 and T = 25°C.

Effect of the initial concentration of ferrous iron

The amount of ferrous ion is one of the main parameters which influences the Fenton and photo-Fenton processes. In this study, to obtain the optimal initial Fe^{2+} concentration, the investigation was carried out in the range of 0.5-8.0 mM Fe^{2+}, at pH 3 and H_2O_2 dosing rate 120 mg·min^{-1}. The results are shown in Fig. 6.

It can be seen that the removal rate of COD clearly increased with the increasing amount of Fe^{2+}, in the range of 0.5–5.0 mM; k_{app} increased from 0.018 to 0.056 ℓ·g^{-1} min^{-1}. It was known that Fe^{2+} had a catalytic decomposition effect on H_2O_2. When the Fe^{2+} concentration increased, the catalytic effect increased accordingly. However, for Fe^{2+} doses higher than 5.0 mM, the COD per cent removal decreased slightly. This decrease was essentially due to competitive consumption of OH· radicals (Eq. (4)).

It is worth noting that, in the Fenton process, the amounts of Fe^{2+} ions should be as low as possible for economic and environmental reasons; high amounts of Fe^{2+} ions might produce a larger quantity of Fe^{3+} sludge. The removal/treatment of the sludge containing Fe^{3+} at the end of the wastewater treatment is expensive and requires a large amount of chemicals and manpower (Ramirez et al., 2007). As shown in the inset of Fig. 6, 5.0 mM Fe^{2+} can be used as an optimum dosage in this work.

Effect of initial pH

The pH affects the oxidation of organic substances both directly and indirectly. The Fenton and photo-Fenton reactions are strongly pH-dependent. The pH value influences the generation of hydroxyl radicals and thus the oxidation efficiency. The effect of pH on the degradation of chlorpyrifos by the Fenton process is shown in Fig. 7. The experiments were carried out at a pH within the range of 2.5-4.0. The optimum pH was found to be about 3, as elucidated by k_{app} values. The degradation decreased at pH values higher than 3.5, because iron precipitated as hydroxide.

Additionally, the oxidation potential of the hydroxyl radical was known to decrease with increasing pH (Lucas and Peres, 2006). Another reason for the inefficient degradation at pH > 3 is the dissociation and auto-decomposition of H_2O_2 (Badawy et al., 2006). For pH values below 2.5, the reaction of hydrogen peroxide with Fe^{2+} is seriously affected causing reduction in hydroxyl radical production, due to hydroxyl-radical scavenging by H^+ ions (Lucas and Peres, 2006).

Effect of temperature

The effect of temperature on the kinetic rate constants, k_{app}, for chlorpyrifos degradation was studied at temperatures of 20, 25, 30, 35, 40 and 45°C, with other test conditions of COD_0 = 1 330 mg·ℓ$^{-1}$, H_2O_2 dosing rate = 120 mg·min^{-1}, $[Fe^{2+}]_0$ = 5.0 mM and pH = 3. The results obtained are shown in Fig. 8, and clearly indicate that k_{app} is significantly affected by reaction temperature, increasing with increasing temperature until an optimal value of 35°C. The decrease of k_{app} at temperatures higher than 40°C is due to the accelerated decomposition of H_2O_2 into oxygen and water. Similar results were reported by Wang (2008).
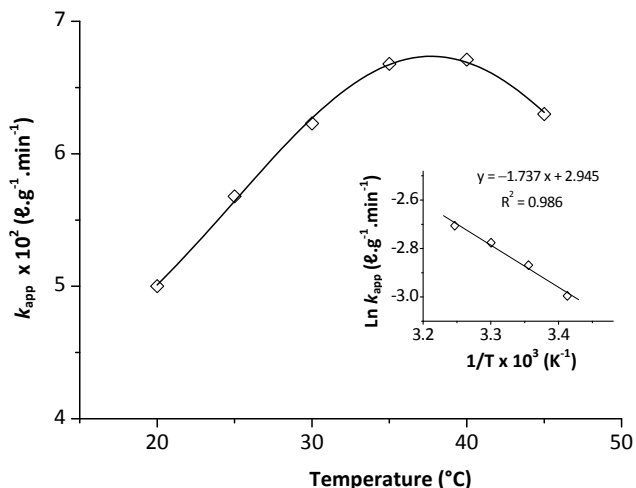
Figure 8
Evolution of k_{app} at different temperatures. The inset shows the plot of Ln k_{app}–(1/T). COD_0 = 1 330 mg·ℓ$^{-1}$; Dosing rate of H_2O_2 120 mg·min^{-1}; $[Fe^{2+}]_0$ = 5.0 mM and pH = 3.

Figure 9
Trend of COD/COD_0 ratio during the oxidation of chlorpyrifos solution by Fenton and solar phto-Fenton reactions. The inset panel shows the fitting of the experimental data to a second-order reaction kinetic model for the 2 processes. Dosing rate of H_2O_2 120 mg·min^{-1}; $[Fe^{2+}]_0$ = 5.0 mM; COD_0 = 1 330 mg·ℓ$^{-1}$; pH = 3 and T = 35°C.

The Arrhenius expression, showing the relationship between the reaction temperature and k_{app} is expressed as follows:

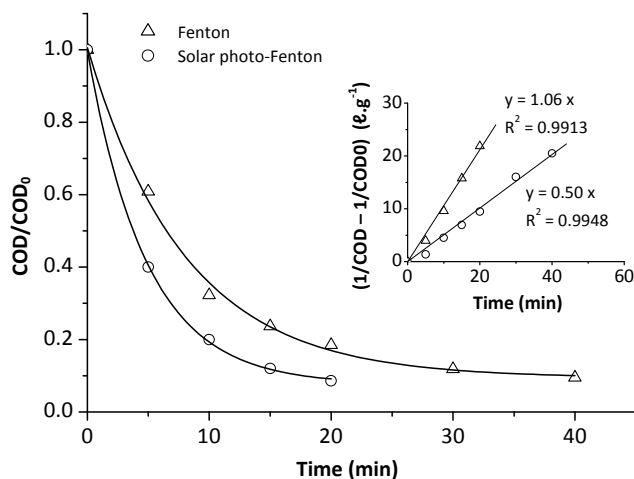$$k_{app} = A \exp\left(-\frac{E_{app}}{RT}\right) \qquad (8)$$

where:
A is the pre-exponential (or frequency) factor
E_{app} is the apparent global activation energy (J·mol^{-1})
R is the ideal gas constant (8.314 J·mol^{-1}·K^{-1})
T is the reaction absolute temperature (K).

Due to the narrow temperature range employed in this study (i.e., 20–35°C), variations of the pre-exponential factors and the apparent activation energies of the empirical Arrhenius expressions of the COD removal may be neglected. The variation of Ln k_{app} versus $1/T$ is plotted in the inset of Fig. 8. Good linear relationships exist between the plot of Ln k_{app} and $1/T$ because the regression coefficient was higher than 0.98. Based on the slope ($-E_{app}/R$) and intercepts (Ln A) of the plot in Fig. 8, E_{app} and A in Arrhenius form (Eq. (8)) are determined, i.e., E_{app} = 14.44 kJ·mol^{-1} and A = 19.01 ℓ·g^{-1}·min^{-1}.

Oxidation of chlorpyrifos by the solar photo-Fenton process

In order to improve the reaction rate and COD abatement efficiency, solutions were subjected to solar radiation using a laboratory-scale reactor (Fig. 2). Fig. 9 shows the trend of the COD/COD_0 ratio during the treatment of chlorpyrifos solution by the 2 processes under the optimum experimental conditions found when using the Fenton process (H_2O_2 = 120 mg·min^{-1}, $[Fe^{2+}]_0$ = 5.0 mM, pH = 3 and T = 35°C). It can be seen that the solar photo-Fenton system needed less time and consequently less H_2O_2 to reach the same COD per cent removal. In fact, under the optimum experimental conditions, the solar photo-Fenton process needed a dose of H_2O_2 50% lower than that used in the Fenton process to remove 90% of COD. The COD removal rate is higher with the solar photo-Fenton process as shown by the k_{app} values in the inset of Fig. 9.

Conclusions

The results of this study indicate that dark Fenton and solar photo-Fenton processes are powerful methods for the degradation of the insecticide chlorpyrifos, but the solar-photo-Fenton process is 50% more efficient than the Fenton process. The degradation rate by the 2 processes can be expressed as a pseudo-second-order reaction with respect to COD. COD removal was influenced by the dosing rate of the hydrogen peroxide (H_2O_2 continuously introduced in the solution), the initial concentration of chlorpyrifos, the amount of iron salt, the pH of solution and the temperature. The optimum conditions were observed at pH 3, with an initial Fe^{2+} concentration of 5.0 mM and H_2O_2 dosing rate of 120 mg·min^{-1}. The experiments carried out within the temperature range 20–45°C showed an optimum COD removal at 35°C, which allowed for computation of the apparent global activation energy (14.44 kJ·mol^{-1}).

The results obtained with this preliminary study suggest that solar photo-Fenton is a promising pre-treatment process for pesticide-containing wastewater.

References

ACERO JL, BENITEZ FJ, GONZALEZ M and BENITEZ R (2002) Kinetics of fenuron decomposition by single-chemical oxidants and combined systems. *Ind. Eng. Chem. Res.* **41** (17) 4225–4232.
ARGUN ME and KARATAS M (2011) Application of Fenton process for decolorization of reactive black 5 from synthetic wastewater: Kinetics and thermodynamics. *Environ. Prog. Sust. Energ.* **30** (4) 540–548.
BADAWY MI, GHALY MY and GAD-ALLAH TA (2006) Advanced oxidation processes for the removal of organophosphorus pesticides from wastewater. *Desalination* **194** (1–3) 166–175.

BOSSMANN SH, OLIVEROS E, GÖB S, SIEGWART S, DAHLEN EP, PAYAWAN L, STRAUB M, WÖRNER M and BRAUN AM (1998) New evidence against hydroxyl radicals as reactive intermediates in the thermal and photochemically enhanced Fenton reactions. *J. Phys. Chem. A* **102** (28) 5542–5550.

BURROWS HD, CANLE LM, SANTABALLA JA and STEENKEN S (2002) Reaction pathways and mechanisms of photodegradation of pesticides. *J. Photochem. Photobiol. B: Biol.* **67** (2) 71–108.

CHIRON S, FERNANDEZ-ALBA A, RODRIGUEZ A and GARCIA-CALVO E (1999) Pesticide chemical oxidation: state-of-the-art. *Water Res.* **34** (2) 366–377.

CUNNIF P (1995) *Official Methods of Analysis of AOAC International* (16th edn.). AOAC international, Arlington. ISBN/ISSN 0935584544.

DERCO J, GOTVAJN AZ, ZAGORC-KONCAN J, ALMASIOVA B and KASSAI A (2010) Pretreatment of landfill leachate by chemical oxidation processes. *Chem. Pap.* **64** (2) 237–245.

DI CORCIA A and MARCHETTI M (1992) Method development for monitoring pesticides in environmental waters: Liquid–solid extraction followed by liquid chromatography. *Environ. Sci. Technol.* **26** (1) 66–74.

ESPLUGAS S, GIMÉNEZ J, CONTRERAS S, PASCUAL E and RODRIGUEZ M (2002) Comparison of different advanced oxidation processes for phenol degradation. *Water Res.* **36** (4) 1034–1042.

GUEDES AMFM, MADEIRA LMP, BOAVENTURA RAR and COSTA CAV (2003) Fenton oxidation of cork cooking wastewater – overall kinetic analysis. *Water Res.* **37** (13) 3061–3069.

HABER F and WEISS J (1934) The catalytic decomposition of hydrogen peroxide by iron salts. *Proc. R. Soc. A* **147** (861) 332–351.

KANG N, LEE DS and YOON J (2002) Kinetic modeling of fenton oxidation of phenol and monochlorophenols. *Chemosphere* **47** (9) 915–924.

KANG YW and HWANG KY (2000) Effects of reaction conditions on the oxidation efficiency in the Fenton process. *Water Res.* **34** (10) 2786–2790.

KOLTHOF IM, SANDELL EB, MEEEHAN EJ and BUCKSTEIN S (1969) *Quantitative Chemical Analysis* (4th edn.). Macmillan, New York.

LIN SH and LO CC (1997) Fenton process for treatment desizing wastewater. *Water Res.* **31** (8) 2050–2056.

LUCAS MS and PERES JA (2006) Decolorization of the azo dye reactive black 5 by Fenton and photo–Fenton oxidation. *Dyes Pigm.* **71** (3) 236–244.

MENG JW, YANG B, ZHANG Y, DONG X and SHU J (2010) Heterogeneous ozonation of suspended malathion and chlorpyrifos particles. *Chemosphere* **79** 394–400.

MODIRSHAHLA N, BEHNAJADY MA and GHANBARY F (2007) Decolorization and mineralization of C.I. acid yellow 23 by Fenton and photo–Fenton processes. *Dyes Pigm.* **73** (3) 305–310.

MURILLO R, SARASA J, LANAO M and OVELLEIRO JL (2010) Degradation of chlorpyrifos in water by advanced oxidation processes. *Water Sci. Technol.* **10** (1) 1–6.

PIGNATELLO JJ (1992) Dark and photoassisted iron(3+)-catalyzed degradation of chlorphenoxy herbicides by hydrogen peroxide. *Environ. Sci. Technol.* **26** (5) 944–951.

RAMIREZ JH, COSTA CA, MADEIRA LM, MATA G, VICENTE MA, ROJAS-CERVANTES ML, LOPEZ-PEINADO AJ and MARTIN-ARANDA RM (2007) Fenton-like oxidation of Orange II solutions using heterogeneous catalysts based on saponite clay. *Appl. Catal. B: Environ.* **71** (1–2) 44–56.

RATANATAMSKUL C and AUESUNTRACHUN P (2009) Removal of COD and colour from old-landfill leachate by Advanced Oxidation Processes. *Int. J. Environ. Waste Manage.* **4** (3–4) 470–480.

SAMET Y, AGENGUI L and ABDELHEDI R (2010) Anodic oxidation of chlorpyrifos in aqueous solution at lead dioxide electrodes. *J. Electroanal. Chem.* **650** 152–158.

TAMIMI M, QOURZAL S, BARKA N, ASSABBANE A and AIT-ICHOU Y (2008) Methomyl degradation in aqueous solutions by Fenton's reagent and the photo–Fenton system. *Sep. Purif. Technol.* **61** (1) 103–108.

WALLING C (1975) Fenton's reagent revisited. *Acc. Chem. Res.* **8** (4) 125–131.

WANG S (2008) A comparative study of fenton and fenton-like reaction kinetics in decolorisation of wastewater. *Dyes Pigm.* **76** 714–720.

XU M, WANG Q and HAO Y (2007) Removal of organic carbon from wastepaper pulp effluent by lab-scale solar photo–Fenton process. *J. Hazard. Mater.* **148** 103–109.